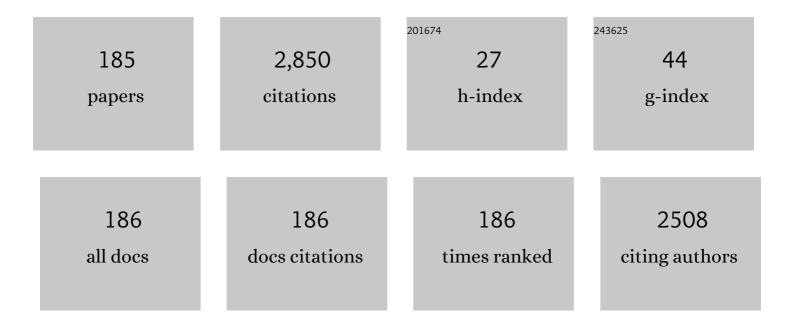
Takeyoshi Sugaya

List of Publications by Year in descending order

Source: https://exaly.com/author-pdf/8987391/publications.pdf Version: 2024-02-01



#	Article	IF	CITATIONS
1	GaAs//CuIn _{1â^'y} Ga _y Se ₂ Three-Junction Solar Cells With 28.06% Efficiency Fabricated Using a Bonding Technique Involving Pd Nanoparticles and an Adhesive. IEEE Journal of Photovoltaics, 2022, 12, 639-645.	2.5	5
2	Integration of Si Heterojunction Solar Cells with III–V Solar Cells by the Pd Nanoparticle Array-Mediated "Smart Stack―Approach. ACS Applied Materials & Interfaces, 2022, 14, 11322-11329.	8.0	9
3	28.3% Efficient Ill–V Tandem Solar Cells Fabricated Using a Tripleâ€Chamber Hydride Vapor Phase Epitaxy System. Solar Rrl, 2022, 6, .	5.8	10
4	Comparison of different passivation layers for GaInAs solar cells grown by solid-source molecular beam epitaxy. Journal of Crystal Growth, 2022, 593, 126769.	1.5	0
5	Perfect Matching Factor between a Customized Double-Junction GaAs Photovoltaic Device and an Electrolyzer for Efficient Solar Water Splitting. ACS Applied Energy Materials, 2022, 5, 8241-8253.	5.1	7
6	Impact of loading topology and current mismatch on current–voltage curves of three-terminal tandem solar cells with interdigitated back contacts. Solar Energy Materials and Solar Cells, 2021, 221, 110901.	6.2	10
7	Epitaxial Lift-Off of Single-Junction GaAs Solar Cells Grown Via Hydride Vapor Phase Epitaxy. IEEE Journal of Photovoltaics, 2021, 11, 93-98.	2.5	11
8	IIIâ€V//Cu _{<i>x</i>} In _{1â^'<i>y</i>} Ga _{<i>y</i>} Se ₂ multijunction solar cells with 27.2% efficiency fabricated using modified smart stack technology with Pd nanoparticle array and adhesive material. Progress in Photovoltaics: Research and Applications, 2021, 29, 887-898.	8.1	21
9	Optoelectronic Inactivity of Dislocations in Cu(In,Ga)Se ₂ Thin Films. Physica Status Solidi - Rapid Research Letters, 2021, 15, 2100042.	2.4	2
10	InGaP/GaAs dualâ€junction solar cells with AlInGaP passivation layer grown by hydride vapor phase epitaxy. Progress in Photovoltaics: Research and Applications, 2021, 29, 1285-1293.	8.1	7
11	Pd-mediated mechanical stack of Ill–V solar cells fabricated via hydride vapor phase epitaxy. Solar Energy, 2021, 224, 142-148.	6.1	8
12	Growth of InGaAs Solar Cells on InP(001) Miscut Substrates Using Solidâ€5ource Molecular Beam Epitaxy. Physica Status Solidi (A) Applications and Materials Science, 2020, 217, 1900512.	1.8	3
13	IIIâ€V//Si multijunction solar cells with 30% efficiency using smart stack technology with Pd nanoparticle array. Progress in Photovoltaics: Research and Applications, 2020, 28, 16-24.	8.1	43
14	Effects of growth interruption on InGaP fabricated via hydride vapor phase epitaxy. Journal of Crystal Growth, 2020, 544, 125712.	1.5	2
15	Cu Nanoparticle Array-Mediated III–V/Si Integration: Application in Series-Connected Tandem Solar Cells. ACS Applied Energy Materials, 2020, 3, 3445-3453.	5.1	9
16	Evaluation of GaAs solar cells grown under different conditions via hydride vapor phase epitaxy. Journal of Crystal Growth, 2020, 537, 125600.	1.5	5
17	High Doping Performance of Sulfur and Zinc Dopants in Tunnel Diodes Using Hydride Vapor Phase Epitaxy. IEEE Journal of Photovoltaics, 2020, 10, 749-753.	2.5	10
18	Analysis of subcell open-circuit voltages of InGaP/GaAs dual-junction solar cells fabricated using hydride vapor phase epitaxy. Japanese Journal of Applied Physics, 2020, 59, SGGF02.	1.5	3

#	Article	IF	CITATIONS
19	Multiple epitaxial lift-off of stacked GaAs solar cells for low-cost photovoltaic applications. Japanese Journal of Applied Physics, 2020, 59, 052003.	1.5	6
20	Application of polydimethylsiloxane surface texturing on III-V//Si tandem achieving more than 2 % absolute efficiency improvement. Optics Express, 2020, 28, 3895.	3.4	8
21	Spectral response measurements of each subcell in monolithic triple-junction GaAs photovoltaic devices. Applied Physics Express, 2019, 12, 102015.	2.4	4
22	Intermediate band formation by InGaAs/GaAs multistacked quantum dots without strain compensation. Journal of Physics: Conference Series, 2019, 1220, 012038.	0.4	1
23	Impact of Nonplanar Panels on Photovoltaic Power Generation in the Case of Vehicles. IEEE Journal of Photovoltaics, 2019, 9, 1721-1726.	2.5	24
24	24.5% efficient GaAs p-on-n solar cells with 120 <i>µ</i> m h ^{â^'1} MOVPE growth. Journal Physics D: Applied Physics, 2019, 52, 105501.	2.8	7
25	Ultrafast growth of InGaP solar cells via hydride vapor phase epitaxy. Applied Physics Express, 2019, 12, 052004.	2.4	15
26	Effects of front InGaP layer thickness on solar cell characteristics in InP/InGaP quantum dot solar cells. Japanese Journal of Applied Physics, 2019, 58, SBBF09.	1.5	2
27	Impact of nanometer air gaps on photon recycling in mechanically stacked multi-junction solar cells. Optics Express, 2019, 27, A1.	3.4	13
28	Improvement of Heterointerface Properties of GaAs Solar Cells Grown With InGaP Layers by Hydride Vapor-Phase Epitaxy. IEEE Journal of Photovoltaics, 2019, 9, 154-159.	2.5	18
29	High throughput MOVPE and accelerated growth rate of GaAs for PV application. Journal of Crystal Growth, 2019, 509, 87-90.	1.5	3
30	Accelerated GaAs growth through MOVPE for low-cost PV applications. Journal of Crystal Growth, 2018, 489, 63-67.	1.5	8
31	Dual-junction GaAs solar cells and their application to smart stacked III–V//Si multijunction solar cells. Applied Physics Express, 2018, 11, 052301.	2.4	14
32	Effect of Series Resistances on Conversion Efficiency of GaAs/Si Tandem Solar Cells With Areal Current-Matching Technique. IEEE Journal of Photovoltaics, 2018, 8, 654-660.	2.5	10
33	Investigation of the open-circuit voltage in wide-bandgap InGaP-host InP quantum dot intermediate-band solar cells. Japanese Journal of Applied Physics, 2018, 57, 04FS04.	1.5	2
34	Enhancement of open-circuit voltage in InGaP solar cells grown by solid source molecular beam epitaxy. Japanese Journal of Applied Physics, 2018, 57, 08RD07.	1.5	5
35	Broadband Reflectance Reduction for Wafer Bonded III-V//Si tandem Cell Using Polydimethylsiloxane -Replicated Surface Texturing. , 2018, , .		0
36	Design and characterization of InGaP-based InP quantum dot solar cells. Japanese Journal of Applied Physics, 2018, 57, 08RF04.	1.5	5

#	Article	IF	CITATIONS
37	Interdot spacing dependence of electronic structure and properties of multistacked InGaAs quantum dots fabricated without strain compensation technique. Japanese Journal of Applied Physics, 2018, 57, 06HE08.	1.5	5
38	Two-step photon absorption in InP/InGaP quantum dot solar cells. Applied Physics Letters, 2018, 113, .	3.3	10
39	Single-crystal Cu(In,Ga)Se ₂ solar cells grown on GaAs substrates. Applied Physics Express, 2018, 11, 082302.	2.4	30
40	Fabrication of GaAs solar cells grown with InGaP layers by hydride vapor-phase epitaxy. Japanese Journal of Applied Physics, 2018, 57, 08RD06.	1.5	14
41	Extremely High-Speed GaAs Growth by MOVPE for Low-Cost PV Application. IEEE Journal of Photovoltaics, 2018, , 1-8.	2.5	8
42	Growth of InGaAsP solar cells and their application to triple-junction top cells used in smart stack multijunction solar cells. Journal of Vacuum Science and Technology B:Nanotechnology and Microelectronics, 2017, 35, .	1.2	10
43	InGaP-based InP quantum dot solar cells with extended optical absorption range. Japanese Journal of Applied Physics, 2017, 56, 04CS06.	1.5	8
44	Feasibility study of two-terminal tandem solar cells integrated with smart stack, areal current matching, and low concentration. Progress in Photovoltaics: Research and Applications, 2017, 25, 255-263.	8.1	18
45	Enhancement of open circuit voltage in InGaAsP-inverted thin-film solar cells grown by solid-source molecular beam epitaxy. Journal of Crystal Growth, 2017, 477, 267-271.	1.5	9
46	Investigation of the properties of semiconductor wafer bonding in multijunction solar cells via metal-nanoparticle arrays. Journal of Applied Physics, 2017, 122, .	2.5	19
47	Investigation of the open-circuit voltage in mechanically stacked InGaP/GaAs//InGaAsP/InGaAs solar cells. Japanese Journal of Applied Physics, 2017, 56, 08MC01.	1.5	12
48	High-efficiency III–V//Si tandem solar cells enabled by the Pd nanoparticle array-mediated "smart stack― approach. Applied Physics Express, 2017, 10, 072301.	2.4	34
49	Effects of substrate miscut on the properties of InGaP solar cells grown on GaAs(001) by solid-source molecular beam epitaxy. Japanese Journal of Applied Physics, 2017, 56, 08MC08.	1.5	3
50	Reduction of bonding resistance of two-terminal III–V/Si tandem solar cells fabricated using smart-stack technology. Japanese Journal of Applied Physics, 2017, 56, 122302.	1.5	4
51	Palladium nanoparticle array-mediated semiconductor bonding that enables high-efficiency multi-junction solar cells. Japanese Journal of Applied Physics, 2016, 55, 025001.	1.5	37
52	Type-II InP quantum dots in wide-bandgap InGaP host for intermediate-band solar cells. Applied Physics Letters, 2016, 108, .	3.3	27
53	Tandem photovoltaic–photoelectrochemical GaAs/InGaAsP–WO ₃ /BiVO ₄ device for solar hydrogen generation. Japanese Journal of Applied Physics, 2016, 55, 04ES01.	1.5	28
54	A proposal for wide-bandgap intermediate-band solar cells using type-II InP/InGaP quantum dots. , 2016, ,		2

4

#	Article	IF	CITATIONS
55	Nanophotonic Devices Based on Semiconductor Quantum Nanostructures. IEICE Transactions on Electronics, 2016, E99.C, 346-357.	0.6	0
56	Carrier dynamics in type-II quantum dots for wide-bandgap intermediate-band solar cells. Proceedings of SPIE, 2016, , .	0.8	5
57	MBE-grown InGaAsP solar cells with 1.0 eV bandgap on InP(001) substrates for application to multijunction solar cells. Japanese Journal of Applied Physics, 2015, 54, 08KE10.	1.5	5
58	Photocatalytic generation of hydrogen by core-shell WO3/BiVO4 nanorods with ultimate water splitting efficiency. Scientific Reports, 2015, 5, 11141.	3.3	464
59	Fabrication of hydrogenated amorphous Si/crystalline Si _{1â^'} <i>_x</i> Ge <i>_x</i> (i>(<i>x</i> ≤0.84) heterojunction solar cells grown by solid source molecular beam epitaxy. Japanese Journal of Applied Physics, 2015, 54, 012301.	1.5	15
60	Investigation of InGaP/(In)AlGaAs/GaAs triple-junction top cells for smart stacked multijunction solar cells grown using molecular beam epitaxy. Japanese Journal of Applied Physics, 2015, 54, 08KE02.	1.5	6
61	Electrical characteristics of amorphous Si:H/crystalline Si0.3Ge0.7 heterojunction solar cells grown on compositionally graded buffer layers. Journal of Crystal Growth, 2015, 425, 162-166.	1.5	2
62	Strain-compensated Ge/Si1â^'C quantum dots with Si mediating layers grown by molecular beam epitaxy. Journal of Crystal Growth, 2015, 425, 167-171.	1.5	1
63	Radiation response of the fill-factor for GaAs solar cells with InGaAs quantum dot layers. , 2014, , .		2
64	Effect of deposition rate on the characteristics of Ge quantum dots on Si (001) substrates. Thin Solid Films, 2014, 557, 80-83.	1.8	2
65	Highly efficient and reliable mechanically stacked multi-junction solar cells using advanced bonding method with conductive nanoparticle alignments. , 2014, , .		5
66	MBE-grown InGaP/GaAs/InGaAsP triple junction solar cells fabricated by advanced bonding technique. , 2014, , .		2
67	InGaP/GaAs tandem solar cells fabricated using solid-source molecular beam epitaxy. Japanese Journal of Applied Physics, 2014, 53, 05FV06.	1.5	17
68	InGaAs quantum dot superlattice with vertically coupled states in InGaP matrix. Journal of Applied Physics, 2013, 114, .	2.5	17
69	In(Ga)As quantum dots on InGaP layers grown by solid-source molecular beam epitaxy. Journal of Crystal Growth, 2013, 378, 430-434.	1.5	17
70	Optical and structural studies of highly uniform Ge quantum dots on Si (001) substrate grown by solid-source molecular beam epitaxy. Journal of Crystal Growth, 2013, 378, 439-441.	1.5	7
71	Miniband formation in InGaAs quantum dot superlattice with InGaP matrix for application to intermediate-band solar cells. , 2013, , .		2
72	InGaP solar cells fabricated using solid-source molecular beam epitaxy. Journal of Crystal Growth, 2013, 378, 576-578.	1.5	27

#	Article	IF	CITATIONS
73	Change in the electrical performance of GaAs solar cells with InGaAs quantum dot layers by electron irradiation. Solar Energy Materials and Solar Cells, 2013, 108, 263-268.	6.2	14
74	Over 20% Efficiency Mechanically Stacked Multi-Junction Solar Cells Fabricated by Advanced Bonding Using Conductive Nanoparticle Alignments. Materials Research Society Symposia Proceedings, 2013, 1538, 167-171.	0.1	10
75	Electrical performance degradation of GaAs solar cells with InGaAs quantum dot layers due to proton irradiation. , 2013, , .		3
76	1.3-Âμm Quantum Dot Distributed Feedback Laser with Half-Etched Mesa Vertical Grating Fabricated by Cl2Dry Etching. Japanese Journal of Applied Physics, 2013, 52, 06GE03.	1.5	2
77	Thermal Conductive Properties of a Semiconductor Laser on a Polymer Interposer. Japanese Journal of Applied Physics, 2013, 52, 04CG05.	1.5	2
78	InGaP-based InGaAs quantum dot solar cells with GaAs spacer layer fabricated using solid-source molecular beam epitaxy. Applied Physics Letters, 2012, 101, .	3.3	32
79	Ultra-high stacks of InGaAs/GaAs quantum dots for high efficiency solar cells. Energy and Environmental Science, 2012, 5, 6233.	30.8	75
80	Analysis of vertical coupling between a 2D photonic crystal cavity and a hydrogenated-amorphous-silicon-wire waveguide. Photonics and Nanostructures - Fundamentals and Applications, 2012, 10, 287-295.	2.0	3
81	Ultra-high stacks of InGaAs quantum dots for high efficiency solar cells. , 2011, , .		2
82	Tunnel current through a miniband in InGaAs quantum dot superlattice solar cells. Solar Energy Materials and Solar Cells, 2011, 95, 2920-2923.	6.2	24
83	Multi-stacked quantum dot solar cells fabricated by intermittent deposition of InGaAs. Solar Energy Materials and Solar Cells, 2011, 95, 163-166.	6.2	56
84	Highly stacked InGaAs quantum dot structures grown with two species of As. Journal of Vacuum Science and Technology B:Nanotechnology and Microelectronics, 2010, 28, C3C4-C3C8.	1.2	19
85	Characteristics of highly stacked quantum dot solar cells fabricated by intermittent deposition of InGaAs. , 2010, , .		3
86	Change in the electrical performance of InGaAs quantum dot solar cells due to irradiation. , 2010, , .		3
87	Design of two-dimensional photonic crystal nanocavities with low-refractive-index material cladding. Journal of Optics (United Kingdom), 2010, 12, 015108.	2.2	4
88	Analysis of two-dimensional photonic crystal L-type cavities with low-refractive-index material cladding. Journal of Optics (United Kingdom), 2010, 12, 075101.	2.2	14
89	Highly Stacked and High-Quality Quantum Dots Fabricated by Intermittent Deposition of InGaAs. Japanese Journal of Applied Physics, 2010, 49, 030211.	1.5	24
90	Miniband formation in InGaAs quantum dot superlattice. Applied Physics Letters, 2010, 97, .	3.3	41

#	Article	IF	CITATIONS
91	Highly stacked and well-aligned In0.4Ga0.6As quantum dot solar cells with In0.2Ga0.8As cap layer. Applied Physics Letters, 2010, 97, 183104.	3.3	50
92	Formation and control of a correlated exciton two-qubit system in a coupled quantum dot. Physical Review B, 2009, 79, .	3.2	7
93	Low threshold current operation of 1.3 µm Quantum Dots Laser with high mirror loss structure. , 2009, , .		Ο
94	1.3 µm Distributed Feedback Laser with Half-Etching Mesa and High-Density Quantum Dots. Japanese Journal of Applied Physics, 2009, 48, 050203.	1.5	3
95	Analysis of Terahertz Oscillator Using Negative Differential Resistance Dual-Channel Transistor and Integrated Antenna. Japanese Journal of Applied Physics, 2009, 48, 04C146.	1.5	3
96	Cascade optical excitation of an artificial exciton molecule in a coupled quantum dot. Physica Status Solidi C: Current Topics in Solid State Physics, 2008, 5, 343-346.	0.8	0
97	1.3-μm quantum dot DFB laser with Half-Etching Mesa and high density QD. , 2008, , .		Ο
98	Optical Control of 2-Qubit Exciton States in a Coupled Quantum Dot. Japanese Journal of Applied Physics, 2008, 47, 3111-3114.	1.5	1
99	Electric-Field Control of Coupled States in Weakly Coupled Quantum Dots. Japanese Journal of Applied Physics, 2008, 47, 2884-2887.	1.5	1
100	Development of high resolution Michelson interferometer for stable phase-locked ultrashort pulse pair generation. Review of Scientific Instruments, 2008, 79, 103101.	1.3	1
101	Suppressed bimodal size distribution of InAs quantum dots grown with an As2 source using molecular beam epitaxy. Journal of Applied Physics, 2008, 104, 083106.	2.5	23
102	An Analysis of Antenna Integrated THz Oscillator Using a Negative Differential Resistance Transistor. IEICE Transactions on Communications, 2008, E91-B, 1800-1805.	0.7	1
103	Exciton Rabi Oscillation in Single Pair of InAs/GaAs Coupled Quantum Dots. Japanese Journal of Applied Physics, 2007, 46, 2626-2628.	1.5	4
104	Laser Characteristics of 1.3-\$mu\$m Quantum Dots Laser With High-Density Quantum Dots. IEEE Journal of Selected Topics in Quantum Electronics, 2007, 13, 1273-1278.	2.9	29
105	Correlated photon emission in a thick barrier coupled quantum dot. Journal of Applied Physics, 2007, 102, 094303.	2.5	5
106	InAs quantum dots array grown with an As2 source on non-planar GaAs substrates. Journal of Crystal Growth, 2007, 301-302, 762-765.	1.5	4
107	InGaAs quantum dots grown with As4 and As2 sources using molecular beam epitaxy. Journal of Crystal Growth, 2007, 301-302, 801-804.	1.5	9
108	Selective excitation of exciton molecule states for the entanglement of excitons in a coupled quantum dots. , 2007, , .		0

#	Article	IF	CITATIONS
109	Electronic structures in single pair of InAsâ^•GaAs coupled quantum dots with various interdot spacings. Journal of Applied Physics, 2006, 99, 033522.	2.5	11
110	Characteristics of 1.3î¼m quantum-dot lasers with high-density and high-uniformity quantum dots. Applied Physics Letters, 2006, 89, 171122.	3.3	25
111	1.3-/spl mu/m InAs quantum-dot laser with high dot density and high uniformity. IEEE Photonics Technology Letters, 2006, 18, 619-621.	2.5	27
112	Negative differential resistance of InGaAs dual channel transistors. Journal of Physics: Conference Series, 2006, 38, 108-111.	0.4	0
113	Realization of 1.3μm InAs quantum dots with high-density, uniformity, and quality. Journal of Crystal Growth, 2006, 295, 162-165.	1.5	16
114	Highly sensitive InGaAsâ^•InAlAs quantum wire photo-FET. Electronics Letters, 2006, 42, 413.	1.0	5
115	Pulse Area Control of Exciton Rabi Oscillation in InAs/GaAs Single Quantum Dot. Japanese Journal of Applied Physics, 2006, 45, 3625-3628.	1.5	8
116	Optical Characteristics of Self-Aligned InAs Quantum Dots in the Presence of GaAs Oval Strain. Japanese Journal of Applied Physics, 2006, 45, 1030-1032.	1.5	1
117	Control of subband energy levels of quantum dots using InGaAs gradient composition strain-reducing layer. Applied Physics Letters, 2006, 88, 261110.	3.3	3
118	InGaAs dual channel transistors with negative differential resistance. Applied Physics Letters, 2006, 88, 142107.	3.3	10
119	Improved optical properties of InAs quantum dots grown with an As2 source using molecular beam epitaxy. Journal of Applied Physics, 2006, 100, 063107.	2.5	35
120	Negative differential resistance of pseudomorphic InGaAs quantum-wire FETs. Journal of Crystal Growth, 2005, 278, 94-97.	1.5	3
121	Highest Density 1.3 µm InAs Quantum Dots Covered with Gradient Composition InGaAs Strain Reduced Layer Grown with an As2Source Using Molecular Beam Epitaxy. Japanese Journal of Applied Physics, 2005, 44, L432-L434.	1.5	29
122	Electronic Structures and Carrier Correlation in Single Pair of Coupled Quantum Dots. Japanese Journal of Applied Physics, 2005, 44, 2647-2651.	1.5	5
123	Observation of Bonding States in Single Pair of Coupled Quantum Dots Using Microspectroscopy. Japanese Journal of Applied Physics, 2005, 44, 2684-2687.	1.5	2
124	1.3â€,μm InAs quantum dots grown with an As[sub 2] source using molecular-beam epitaxy. Journal of Vacuum Science & Technology an Official Journal of the American Vacuum Society B, Microelectronics Processing and Phenomena, 2005, 23, 1243.	1.6	25
125	Enhanced peak-to-valley current ratio in InGaAsâ^•InAlAs trench-type quantum-wire negative differential resistance field-effect transistors. Journal of Applied Physics, 2005, 97, 034507.	2.5	27
126	Observation of interdot correlation in single pair of electromagnetically coupled quantum dots. Applied Physics Letters, 2005, 87, 182103.	3.3	16

#	Article	IF	CITATIONS
127	Observation of exciton molecule consisting of two different excitons in coupled quantum dots. Applied Physics Letters, 2005, 87, 253110.	3.3	13
128	Coherent Control of Exciton in a Single Quantum Dot Using High-Resolution Michelson Interferometer. Japanese Journal of Applied Physics, 2004, 43, 6093-6096.	1.5	4
129	Photoconductive characteristics in a trench-type InGaAs quantum-wire field effect transistor. Journal of Vacuum Science & Technology an Official Journal of the American Vacuum Society B, Microelectronics Processing and Phenomena, 2004, 22, 1523.	1.6	0
130	Optical Characteristics of InAs/GaAs Double Quantum Dots Grown by MBE with the Indium-Flush Method. Japanese Journal of Applied Physics, 2004, 43, 2083-2087.	1.5	12
131	V-grooved InGaAs quantum-wire FET fabricated under an As2 flux in molecular-beam epitaxy. Journal of Crystal Growth, 2003, 251, 843-847.	1.5	1
132	Pseudomorphic InGaAs quantum-wire FETs with negative differential resistance. Superlattices and Microstructures, 2003, 34, 479-484.	3.1	0
133	Magneto-conductance fluctuations in a V-grooved GaAs quantum-wire. Physica E: Low-Dimensional Systems and Nanostructures, 2003, 19, 102-106.	2.7	1
134	Negative differential resistance effects of trench-type InGaAs quantum-wire field-effect transistors with 50-nm gate-length. Applied Physics Letters, 2003, 83, 701-703.	3.3	15
135	Electron Transport Properties in a GaAs/AlGaAs Quantum Wire Grown on V-Grooved GaAs Substrate by Metalorganic Vapor Phase Epitaxy. Japanese Journal of Applied Physics, 2003, 42, 2399-2403.	1.5	7
136	Experimental studies of the electron–phonon interaction in InGaAs quantum wires. Applied Physics Letters, 2002, 81, 727-729.	3.3	30
137	Quantum-interference characteristics of a 25 nm trench-type InGaAs/InAlAs quantum-wire field-effect transistor. Applied Physics Letters, 2002, 80, 434-436.	3.3	30
138	Trench-type InGaAs quantum-wire field effect transistor with negative differential conductance fabricated by hydrogen-assisted molecular beam epitaxy. Journal of Vacuum Science & Technology an Official Journal of the American Vacuum Society B, Microelectronics Processing and Phenomena, 2002, 20, 1192.	1.6	1
139	Electron–phonon scattering in an etched InGaAs quantum wire. Physica B: Condensed Matter, 2002, 314, 99-103.	2.7	8
140	Application of narrow band-gap materials in nanoscale spin filters. Physica B: Condensed Matter, 2002, 314, 230-234.	2.7	8
141	High-average-power self-starting mode-locked Ti:sapphire laser with a broadband semiconductor saturable-absorber mirror. Applied Optics, 2001, 40, 3539.	2.1	7
142	Gate-length dependence of negative differential resistance in ridge-type InGaAs/InAlAs quantum wire field-effect transistor. Solid-State Electronics, 2001, 45, 1099-1105.	1.4	2
143	A diode-pumped, self-starting, all-solid-state self-mode-locked Cr:LiSGAF laser. Optics and Laser Technology, 2001, 33, 71-73.	4.6	3
144	Terahertz Electromagnetic Wave Generation from Quantum Nanostructure. Japanese Journal of Applied Physics, 2001, 40, 3012-3017.	1.5	10

#	Article	IF	CITATIONS
145	Observation of negative differential resistance of a trench-type narrow InGaAs quantum-wire field-effect transistor on a (311)A InP substrate. Applied Physics Letters, 2001, 78, 2369-2371.	3.3	13
146	Trench-type narrow InGaAs quantum wires fabricated on a (311)A InP substrate. Applied Physics Letters, 2001, 78, 76-78.	3.3	24
147	Quasi-one-dimensional transport characteristics of ridge-type InGaAs quantum-wire field-effect transistors. Applied Physics Letters, 2001, 79, 371-373.	3.3	11
148	<title>Ultrafast manipulation of coherent excitons using ultrashort-pulse sequences prepared by frequency domain shaping</title> . , 2000, , .		0
149	Low-loss broadband semiconductor saturable absorber mirror for mode-locked Ti:sapphire lasers. Optics Communications, 2000, 176, 171-175.	2.1	20
150	1.25-MW peak-power Kerr-lens mode-locked Ti:sapphire laser with a broadband semiconductor saturable-absorber mirror. Optics Communications, 2000, 183, 159-163.	2.1	5
151	Gold-reflector-based semiconductor saturable absorber mirror for femtosecond mode-locked Cr4+:YAG lasers. Applied Physics B: Lasers and Optics, 2000, 70, S59-S62.	2.2	14
152	Gate-Length Dependence of Negative Differential Resistance in InGaAs/InAlAs Quantum Well Field-Effect Transistor. Japanese Journal of Applied Physics, 2000, 39, 6152-6156.	1.5	5
153	Negative differential resistance of a ridge-type InGaAs quantum wire field-effect transistor. Journal of Vacuum Science & Technology an Official Journal of the American Vacuum Society B, Microelectronics Processing and Phenomena, 2000, 18, 1680.	1.6	2
154	Ultrafast Coherent Control of Excitons Using Pulse-Shaping Technique. Japanese Journal of Applied Physics, 2000, 39, 2347-2352.	1.5	15
155	Observation of N-shaped negative differential resistance in ridge-type InGaAs/InAlAs quantum wire field-effect transistor. Physica B: Condensed Matter, 1999, 272, 117-122.	2.7	11
156	Quasi-quantum-wire field-effect transistor fabricated by composition-controlled, selective growth in molecular beam epitaxy. Journal of Crystal Growth, 1999, 201-202, 833-836.	1.5	2
157	Self-starting mode-locked Cr^4+:YAG laser with a low-loss broadband semiconductor saturable-absorber mirror. Optics Letters, 1999, 24, 1768.	3.3	34
158	<title>Coherent control of excitons in single and coupled quantum wells</title> . , 1999, , .		0
159	Femtosecond Pulse Generation around 1.3 µm Employing Semiconductor Saturable Absorber Mirrors (SESAM). Springer Series in Photonics, 1999, , 284-292.	0.8	0
160	Effects of As2 flux for fabrication of GaAs/AlGaAs quantum wires on V-grooved substrates in molecular beam epitaxy. Journal of Crystal Growth, 1998, 186, 27-32.	1.5	11
161	Diode-pumped Cr:forsterite laser mode locked by a semiconductor saturable absorber. Applied Optics, 1998, 37, 7080.	2.1	7
162	Femtosecond Cr:forsterite laser diode pumped by a double-clad fiber. Optics Letters, 1998, 23, 129.	3.3	17

#	Article	IF	CITATIONS
163	Broadband semiconductor saturable-absorber mirror for a self-starting mode-locked Cr:forsterite laser. Optics Letters, 1998, 23, 1465.	3.3	43
164	Operation of InGaAs quasi-quantum-wire FET fabricated by selective growth using molecular beam epitaxy. Electronics Letters, 1998, 34, 926.	1.0	14
165	High-power self-starting femtosecond Cr:forsterite laser. Electronics Letters, 1998, 34, 559.	1.0	13
166	THz-radiation Generation from an Intracavity Saturable Bragg Reflector in a Magnetic Field. Japanese Journal of Applied Physics, 1998, 37, L125-L126.	1.5	11
167	Effects of As2Flux and Atomic Hydrogen Irradiation for Growth of InGaAs Quantum Wires by Molecular Beam Epitaxy. Japanese Journal of Applied Physics, 1998, 37, 1497-1500.	1.5	22
168	Femtosecond Cr:forsterite laser diode pumped by a double-clad fiber. , 1998, , .		0
169	All-solid-state, THz-radiation source using a femtosecond mode-locked laser with a saturable Bragg reflector in a magnetic field. , 1998, , .		0
170	All-Solid-State, THz Radiation Source Using a Saturable Bragg Reflector in a Femtosecond Mode-Locked Laser. Japanese Journal of Applied Physics, 1997, 36, L560-L562.	1.5	14
171	Fabrication of InGaAs quantum wire structures by As/sub 2/ flux in molecular beam epitaxy. , 1997, , .		0
172	Difference in Diffusion Length of Ga Atoms underAs2andAs4Flux in Molecular Beam Epitaxy. Japanese Journal of Applied Physics, 1997, 36, 5670-5673.	1.5	20
173	Self-starting mode-locked femtosecond forsterite laser with a semiconductor saturable-absorber mirror. Optics Letters, 1997, 22, 1006.	3.3	63
174	Femtosecond Cr:forsterite laser with mode locking initiated by a quantum-well saturable absorber. IEEE Journal of Quantum Electronics, 1997, 33, 1975-1981.	1.9	41
175	Atomic Hydrogen-Assisted GaAs Molecular Beam Epitaxy. Japanese Journal of Applied Physics, 1995, 34, 238-244.	1.5	22
176	Low Temperature Surface Cleaning of InP by Irradiation of Atomic Hydrogen. Japanese Journal of Applied Physics, 1993, 32, L287-L289.	1.5	47
177	Fabrication of GaAs Quantum Wire Structures by Hydrogen-Assisted Molecular Beam Epitaxy. Japanese Journal of Applied Physics, 1993, 32, L1834-L1836.	1.5	16
178	Selective Growth of GaAs by Molecular Beam Epitaxy. Japanese Journal of Applied Physics, 1992, 31, L713-L716.	1.5	46
179	Investigation of growth mechanism of GaAs in molecular beam epitaxy with atomic hydrogen irradiation. Applied Surface Science, 1992, 60-61, 251-255.	6.1	3
180	Low-Temperature Substrate Annealing of Vicinal Si(100) for Epitaxial Growth of GaAs on Si. Japanese Journal of Applied Physics, 1991, 30, 3774-3776.	1.5	27

#	Article	IF	CITATIONS
181	Low-Temperature Cleaning of GaAs Substrate by Atomic Hydrogen Irradiation. Japanese Journal of Applied Physics, 1991, 30, L402-L404.	1.5	155
182	Anisotropic Lateral Growth of GaAs by Molecular Beam Epitaxy. Japanese Journal of Applied Physics, 1989, 28, L1077-L1079.	1.5	44
183	Negative differential resistance of InGaAs quantum wire FET. , 0, , .		0
184	Fabrication of InGaAs quantum-wire field-effect transistor by selective growth in molecular beam epitaxy. , 0, , .		0
185	Negative differential resistance in trench-type narrow InGaAs quantum wire. , 0, , .		0